Available online at www.sciencedirect.com

ScienceDirect

Energy Procedia 114 (2017) 6685 – 6697

Energy Procedia

13th International Conference on Greenhouse Gas Control Technologies, GHGT-13, 14-18 November 2016, Lausanne, Switzerland

# Assessment of Fracture Propagation in Pipelines Transporting Impure $CO_2$ Streams

Sergey B. Martynov[a], Reza H. Talemi[b], Solomon Brown[a,c], and Haroun Mahgerefteh[a,*]

[a]*Department of Chemical Engineering, University College London, London, WC1E7JE*
[b]*ArcelorMittal Global R&D Gent OCAS N.V., Pres. J.F. Kennedylaan 3, 9060 Zelzate, Belgium*
[c]*Present address: Department of Chemical and Biological Engineering, The University of Sheffield, S1 3JD, UK*

**Abstract**

Running fractures are considered as most dangerous catastrophic mode of failure of high-pressure transportation pipelines. This paper describes methodology for coupled modelling of an outflow, heat transfer and crack propagation in pipelines. The methodology is validated and applied to investigate the ductile fracture propagation in pipelines transporting impure $CO_2$ streams to provide recommendations for the fracture control. To assess the propensity of pipelines to brittle fractures, the temperature distribution in the pipe wall in the vicinity of a crack is simulated for various conditions of heat transfer relevant to both overground and buried pipelines.

© 2017 The Authors. Published by Elsevier Ltd. This is an open access article under the CC BY-NC-ND license (http://creativecommons.org/licenses/by-nc-nd/4.0/).
Peer-review under responsibility of the organizing committee of GHGT-13.

*Keywords:* High-pressure transportation pipelines; Ductile fracture; Brittle fracture; $CO_2$

## 1. Introduction

It is widely accepted that economically viable long-distance onshore transportation of large quantities of gases and liquids in petrochemical industry and, recently, carbon dioxide ($CO_2$) in Carbon Capture and Sequestration projects, can be achieved using pressurized pipelines [1,2]. In cases where such pipelines are passing close to

* Corresponding author. Tel./Fax: +4420 7679 3835
*E-mail address:* h.mahgerefteh@ucl.ac.uk

1876-6102 © 2017 The Authors. Published by Elsevier Ltd. This is an open access article under the CC BY-NC-ND license (http://creativecommons.org/licenses/by-nc-nd/4.0/).
Peer-review under responsibility of the organizing committee of GHGT-13.
doi:10.1016/j.egypro.2017.03.1797

residential areas, their safety becomes of primary concern for the pipeline design, which should ensure minimal risks posed by the release of a toxic, as it would be, e.g. in the case of $CO_2$, or flammable inventory, as in the case of hydrocarbons, in a hypothetical scenario of the pipeline accidental failure. One of the most dangerous failure scenarios is associated with the pipeline running fractures, damaging long pipeline sections and resulting with rapid releases of large amounts of the inventory. For example, a 0.23 m diameter 250 m long pipeline operating at 80 bar pressure would typically contain *ca* 4 tons of dense-phase $CO_2$ fluid, which in case of the pipeline full-bore rupture (FBR) will be released in *ca* 20 s [3]. In order to reduce the risks of the pipeline running fractures, the pipeline material, diameter and wall thickness, as well as mitigation measures (e.g. placement of the pipeline crack arrestors and using emergency isolation valves) are carefully considered in the design relying on predictions using mathematical models of fracture propagation and arrest. For this purpose various approaches have been developed to predict the pipeline failure in both ductile and brittle fracture modes.

**Nomenclature**

| | |
|---|---|
| $A$ | Flow area, $m^2$ |
| $C_v$ | Full-size Charpy V-notch (CVN) energy, J |
| $D$ | Pipeline internal diameter, m |
| $e$ | Fluid specific energy, J/kg |
| $E$ | Elastic modulus, MPa |
| $h$ | Heat transfer coefficient, $W/m^2/K$ |
| $k_w$ | Pipe wall thermal conductivity, W/m/K |
| $u$ | Flow velocity, m/s |
| $u_{cr}$ | Crack tip velocity, m/s |
| $P$ | Fluid pressure, Pa |
| $P_{cr}$ | Crack tip pressure, MPa |
| $P_{arr}$ | Crack arrest pressure, MPa |
| $q_w$ | Heat flux, $W/m^2/K$ |
| $t$ | Time, s |
| $T$ | Temperature, $^oC$ |
| $x$ , $y$ , $z$ | Orthogonal coordinates, m |

**Greek symbols**

| | |
|---|---|
| $\delta_w$ | Pipeline wall thickness, m |
| $\rho$ | Fluid density, kg/m3 |
| $\sigma_f$ | Flow stress, MPa |
| $\sigma_{YS}$ | Yield stress, MPa |
| $\sigma_{TS}$ | Tensile stress, MPa |

Ductile fractures in pipelines may develop from small cracks initiated by the loss of material of the pipe wall due to corrosion or third-party damage. If the pressure in the pipe near the crack location exceeds the ability of the pipe

wall material to resist, the crack may start propagating along the pipeline. Simultaneously, the decrease in pressure in the remaining fluid inventory caused by the release of fluid will eventually bring the crack to rest.

In the past, ductile fracture propagation in pipelines has been modelled based on empirical methodologies, such as the Battelle Two Curve (BTC) method [4] and the High Strength Line Pipe Committee (HLP) model [5]. The BTC methodology provides a criterion for the fracture propagation based on comparison of velocities of the decompression wave in fluid and the running crack, assuming the two phenomena are fully decoupled. Combining the BTC methodology with a model for the history of pipeline decompression enabled prediction of the fracture propagation distance [6,7].

Recently, in order to more accurately predict the crack tip pressure variation during the pipeline decompression, several authors have developed models accounting for two-way coupling between the outflow and crack propagation [8–12]. These studies commonly use the Homogeneous Equilibrium Mixture (HEM) model to describe the decompression flow in the pipe [13] and various approaches to model the fracture mechanics and the dynamic interaction between the propagating crack and the flow. In particular, Mahgerefteh *et al* [10], developed a methodology for simulation of a running ductile fracture in pipelines transporting flashing fluids based on coupling of a FBR HEM flow model predicting the pipeline decompression and an HLP model predicting the crack propagation speed as a function of the crack tip pressure. The model developed was validated against the experimental data [5,14,15] and applied to evaluate the scenarios of fracture propagation in pipelines carrying industrial $CO_2$ streams of various purity. The study confirmed that in comparison with the natural gas, $CO_2$ poses higher risks of ductile fracture in pipelines, which was explained by relatively high vapor pressure of $CO_2$ [16]. It was also shown that a decrease in the boiling point of $CO_2$ caused by the presence of impurities resulted in longer ductile fractures [10]. Aursand *et al* [9] have simulated the pipeline deformations and fracture using an elasto-plastic Finite Element Model (FEM) with shell elements and a local ductile crack propagation criterion, while the loss of fluid through a crack along the pipe was simulated using a 'straw model' [17]. Comparison of the model predictions with the results obtained using uncoupled BTC and HLP models showed that the latter may not give conservative estimate of the ductile fracture propagation in $CO_2$ pipelines [9]. Similar conclusion can also be derived from the results of simulations performed in CO2QUEST project [18], where the ductile fracture propagation in $CO_2$ pipelines was described using HLP model and a modified Bai-Wierzbicki ductile failure model implemented in structural mechanics FEM code [19]. However, despite the recent progress in computational modelling of the ductile fracture propagation in $CO_2$ pipelines, the implications of the presence of impurities in the transported stream for the pipeline design remains unclear.

In contrast to ductile fractures, the brittle fractures in pipelines could propagate if the stress intensity at the crack tip falls below the critical level of the material fracture toughness, which may vary dramatically near the Ductile to Brittle Transition Temperature (DBTT). As such, to prevent the pipelines failure in brittle mode, the pipelines are designed to guarantee high material toughness for the range of operating temperatures. While the brittle fractures are commonly not of concern for modern gas transportation pipelines, it has been recognized for fluids with low boiling points, such as ethylene and carbon dioxide, the near-adiabatic expansion of the fluid from a leak in a buried pipeline may result in significant drop of the pipe wall temperature, causing embrittlement of the pipeline steel, and potentially leading to escalation of small leak into a more catastrophic full-bore rupture [20,21]. In order to quantify the temperature variation around a small puncture hole in a pipeline transporting dense-phase ethylene Saville *et al* [22] have applied a vessel blow-down model. They have concluded that following the pipeline decompression to the fluid saturation pressure the rate of the outflow and temperature drop at the puncture hole were significantly affected by location of the puncture hole relative to the liquid level in the pipe. Mahgerefteh and Atti [20] have applied an HEM flow model to examine the temperature variation upstream a small circular puncture in an over-ground pipeline transporting natural gas, showing that emergency isolation of the pipeline may extend the area near the rupture hole where the temperatures may fall below the DBTT of the pipeline steel. In a recent study by Talemi *et al* [23] the brittle fracture propagation was simulated using an extended FEM model for a worst-case scenario assuming that the pipe wall has reached a temperature below DBTT level as a result of prolonged exposure to a cold fluid expanding from the initial crack. While the study has focused on the validation of the brittle crack propagation model and its dynamic coupling with the pipeline decompression model, the fracture propagation and heat transfer in the pipeline were thermally decoupled. This assumption leads to overestimation of the crack propagation velocity and the crack arrest distances predicted by the model, potentially leading to over-design of the pipeline**.** One of the

tasks of the recently commenced Qatar National Foundation project [24] is to experimentally validate the pipeline fracture model accounting for the impact of the fluid expansion cooling on the pipe wall temperature and, hence, the required pipe material fracture toughness.

In a summary, the above brief literature review shows that despite the progress in modelling ductile fracture propagation in pipes, the modelling of brittle failure of pipelines have not been fully addressed yet. This can partially be attributed to complex nature of the brittle crack propagation phenomena, which requires coupling of the models of transient decompression of the fluid in the pipe, deformations and crack propagation in the pipeline steel, and importantly, the heat transfer between the pipe wall and the streams inside and outside the pipe.

Aiming to address the above issues, the present study, performed in the course of CO2QUEST project [18], is focused on the development of a methodology for full dynamic and thermal coupling between the outflow and the pipe wall rupture models to enable accurate prediction of a wide range of scenarios of accidental failure of high-pressure pipelines transporting dense-phase and supercritical fluids.

The paper is organized as follows. Section 2 describes Methodology, covering the fluid-structure interaction (FSI) model for coupling the models of fluid flow and crack propagation and a model of heat transfer through the pipe wall. This is followed by Section 3.1, presenting the results of analysis of the impact of typical impurities present in $CO_2$ streams captured from fossil-fuel burning power plants on the ductile fracture propagation and arrest. In Section 3.2, aiming to define the range of conditions that could lead to significant cooling of the pipe wall leading to initiation of a running brittle fracture, the temperature distribution in the vicinity of the crack is analyzed for hypothetical heat transfer conditions inside and outside the pipe wall. Conclusions are stated in Section 4.

## 2. Methodology

### *2.1. Fluid-Structure Interaction (FSI) modelling*

The running ductile fracture is a transient phenomenon, which involves dynamic coupling of the pipe wall crack propagation and the pipeline decompression. In particular, as a result of fracture propagation, the length of un-fractured section of the pipeline decreases. In turn, as the pressure in the pipeline drops during the decompression, the driving force for the pipe wall deformations and fracture weakens, while speed of the fracture propagation reduces. In order to model this coupled behaviour, the FSI concept is applied in the present study. This concept assumes that running pipeline fracture is a propagating mode of full-bore rupture of a pipe, which can be modelled as advection of an expansion in the pipe cross-section area along the pipe at a speed of a crack, $u_{cr}$ (Fig. 1).

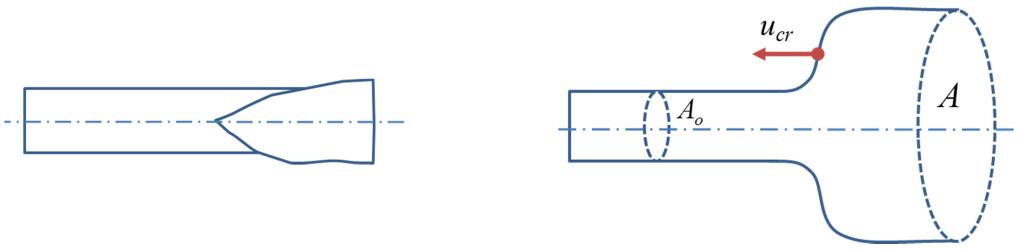


Fig. 1. Schematic representation of the pipeline fracture (a) and the corresponding variation of the effective flow area in the model (b).

The fracture speed $u_{cr}$ is governed by the structural mechanics model as described in Section 2.3 and serves as one of the coupling parameters of the FSI model. The other coupling parameters of the model include the bulk fluid pressure, which can be predicted using the pipeline decompression model presented in Section 2.2, and the

temperature distribution around the fracture tip as predicted by the crack propagation model of Section 2.3. Further details of the dynamic FSI coupling algorithm are described in Talemi *et al* [23].

### *2.2. Pipeline outflow model*

To predict the pertinent fluid properties within the pipeline during its decompression resulting from puncture or FBR, the Computational Fluid Dynamics (CFD) model has been developed for the one-dimensional transient compressible HEM flow [13]. This model accounts for all the important processes taking place during depressurization, including heat transfer, friction, expansion wave propagation and multi-phase flow. The HEM assumption implies thermal and dynamic equilibrium between saturated liquid and vapor phases, and approximately neglects non-equilibrium and heterogeneous nature of the flow. Preliminary studies confirmed that HEM can predict well the history of decompression of $CO_2$ pipelines [25], and therefore HEM was chosen as the most suitable model for the purpose of development and testing of the FSI methodology in the present study.

A set of equations describing the HEM flow in a variable cross-section are pipe includes advection equation for the pipe cross-sectional area and the mass, momentum and energy conservation equations:

$$\frac{\partial A}{\partial t} + u_{cr}\frac{\partial A}{\partial z} = 0 \tag{1}$$

$$\frac{\partial A\rho}{\partial t} + \frac{\partial A\rho u}{\partial z} = 0 \tag{2}$$

$$\frac{\partial A\rho u}{\partial t} + \frac{\partial A(\rho u^2 + P)}{\partial z} = P\frac{\partial A}{\partial z} - \frac{2 f_w A \rho u^2}{D} \tag{3}$$

$$\frac{\partial AE}{\partial t} + \frac{\partial Au(E+P)}{\partial z} = \frac{4Aq_{w,in}}{D} - \frac{2 f_w A \rho u^3}{D} \tag{4}$$

where $\rho$, $u$ and $P$ are respectively the mixture density, velocity and pressure, which are functions of time, $t$, and space, $z$, $D$ and $A$ are respectively the local instantaneous pipeline diameter and cross-section area, $q_{w,in}$ is the heat flux at the internal side of the pipe wall, $f_w$ is the Fanning friction factor calculated using Chen's correlation [26], and $E = \rho\left(e + u^2/2\right)$ is the total energy of the mixture per unit volume, while $e$ and $\rho$ are respectively the specific internal energy and density of the fluid, which are calculated using interpolation tables built using PC-SAFT equation of state [27,28].

The numerical solution of the set of quasi-linear hyperbolic equations (1) – (4), closed by initial and boundary conditions for the flow at either end of the pipeline, is obtained using the finite-volume method [29]. Details of the implementation of this method were previously described [30] and for brevity are omitted here.

### *2.3. Pipeline fracture model*

Comparison of the various ductile fracture propagation models performed in CO2QUEST project [18] showed that the HLP model generally underestimates the fracture propagation distance, but in comparison with other more rigorous FEM-based fracture mechanics models [19], provides an efficient and robust method for predicting the pipeline fracture propagation and arrest. For this reason, the HLP model was chosen in the present work to study the incremental impact of impurities on the ductile facture propagation in $CO_2$ pipelines.

In the HLP model the crack tip velocity, $u_{cr}$, is calculated using an empirical equation based on the Drop Weight Tear Test (DWTT) energy tests data [5]:

$$u_{cr} = 0.67 \frac{\sigma_f}{\sqrt{J_{DWTT} / A_p}} \left( \frac{P_{cr}}{P_{arr}} - 1 \right)^{0.393} \tag{5}$$

where $J_{DWTT} = 3.29 \delta_w^{1.5} C_v^{0.544}$ is the material fracture resistance, $\sigma_f = 0.5(\sigma_{YS} + \sigma_{TS})$ is the flow stress, and $P_{cr}$ is the crack arrest pressure defined by the following empirical equation:

$$P_{arr} = 0.382 \frac{\delta_w}{D} \cdot \sigma_f \cdot \cos^{-1} \exp\left( -3.81 \cdot 10^7 \frac{J_{DWTT} / A_p}{\sigma_f^2 \sqrt{D \cdot \delta_w}} \right) \tag{6}$$

In this equation $A_p$ is the ligament area of a pre-cracked specimen.

Given relatively high expected speeds of propagating ductile fractures, and relatively little time for the heat exchange between the fluid and the pipe wall, the latter can be expected to have relatively little impact on the temperature of the pipe wall. As such, the temperature of the pipe wall is assumed to remain constant in the ductile fracture propagation model.

### *2.4. Heat transfer model*

In order to resolve the temperature variation in the pipe wall in vicinity of the rupture hole (Fig. 2, *a*), the heat conduction equation is applied [31]. Given a relatively small size of the hole, and expected slow variation in the flow during the release, the analysis is performed for steady-state heat transfer conditions. The heat conduction equation is then solved subject to the boundary conditions at the pipe wall. In particular, the convective cooling boundary conditions are applied to define the heat fluxes at the internal and external surfaces of the pipe (Fig. 2, *a*):

$$q_{w,in} \equiv -k_w \nabla T_{w,in} = h_{in} (T_{in} - T_{w,in}) \tag{8}$$

$$q_{w,ext} \equiv -k_w \nabla T_{w,ext} = h_{ext} (T_{w,ext} - T_{ext}) \tag{9}$$

where $T_{in}$ and $T_{ext}$ are respectively the temperatures of the bulk fluids inside and outside the pipe, $T_{w,in}$ and $T_{w,ext}$ are the temperatures at the internal and external surfaces of the pipe, while $h_{in}$ and $h_{ext}$ are the heat transfer coefficients which are assumed to be spatially uniform.

At the rupture hole, where the flow can be expected to be choked, resulting in a high-intensity flash evaporation, the wall temperature is set to a boiling temperature of the fluid at the choked pressure, which in the turn can be predicted by the pipeline decompression model of Section 2.2.

The heat conduction problem was solved using a finite element method in ABAQUS standard v. 6.13 [32]. Fig. 2, *b* shows the FEM mesh built for one quarter of the pipe wall segment confined between the *x*-*y* and *y*-*z* symmetry planes.

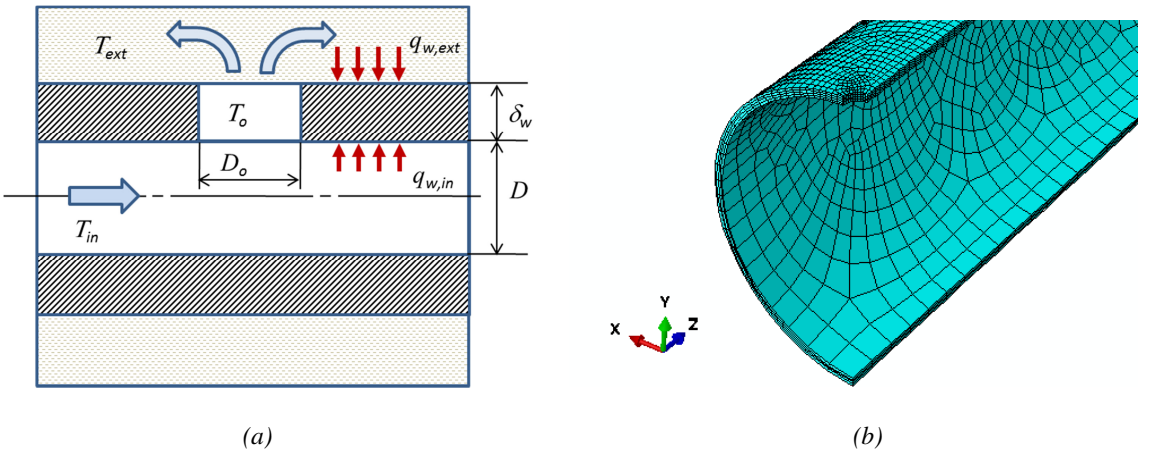


*(a)* *(b)*

Fig. 2. Schematic representation of an outflow and heat transfer through the pipe wall near a puncture hole *(a)*, and FEM discretization of the pipe wall section for the heat transfer analysis in ABAQUS *(b)*.

## 3. Results and discussion

### *3.1. Ductile fractures – Impact of $CO_2$ stream impurities*

In the present section, the impact of impurities on the ductile fracture propagation in $CO_2$ transportation pipelines is performed for $CO_2$ mixtures with $N_2$, $O_2$, $H_2$, Ar, $H_2S$ and $CH_4$, which are among the major components found in $CO_2$ streams captured using post-combustion, pre-combustion and oxy-fuel technologies [33]. For the sake of example, the simulations were performed for an air-exposed X65 steel pipeline of an internal diameter of 0.5905 m, the wall thickness 9.45 mm, and the CVN fracture toughness $C_v$ of 50 J. The initial pressure was set to 80 bar, while the initial fluid temperature has been varied in the range from 0 to 45 $^oC$ relevant to conditions of $CO_2$ capture and pipeline transport. In the CFD simulations the 20 m long section of the pipe was discretized uniformly into 500 cells, and the FSI coupling time step was set to 0.1 ms.

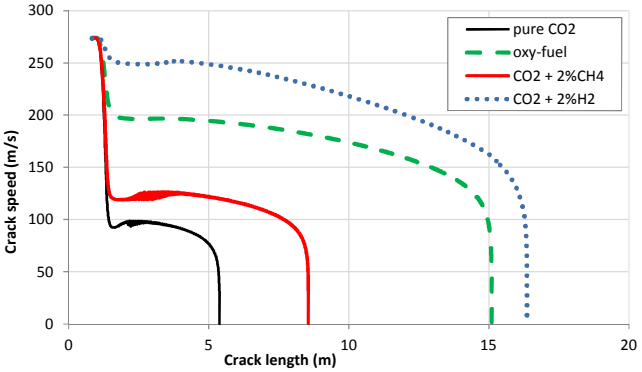


Fig. 3. Variation of the crack propagation speed with the crack length as predicted by the model coupled HLP-CFD for various $CO_2$ streams initially at 80 bar and 15 $^oC$, in a X65 steel pipe of 0.5905 m diameter, 9.45 mm wall thickness and $C_v$=50 J.

Fig. 3 shows the variation of the crack propagation speed with the crack length, as predicted for high-purity $CO_2$ and its mixtures with impurities, namely binary mixture of $CO_2$ with 2% $CH_4$ (v/v) and $H_2$, and quaternary $CO_2$ mixture of 96.8% (v/v) purity containing 1.6% (v/v) of $N_2$, 1.2% (v/v) of $O_2$ and 0.4% (v/v) of Ar, representative of of a double-flash oxy-fuel stream. As can be seen from Fig. 3, the variation of the crack propagation speed with distance is characterized by the following trends:

1. At the initiation of the crack, the crack length is set to 1.2 m, while the crack speed is around 275 m/s as predicted by the model for the initial pressure of 80 bar, independent of the $CO_2$ mixture composition.
2. Immediately after the crack initiation the crack speed drops dramatically and stabilizes at a certain level which depends on the $CO_2$ stream composition and purity. In particular, in case of pure $CO_2$, the crack speed stabilizes at *ca* 100 m/s, while for $CO_2$ containing 2% $CH_4$ , 2% $H_2$ and the oxy-fuel mixture, the crack speed stabilizes around 120, 250 and 200 m/s respectively. The level at which the crack speed temporarily stabilizes corresponds to the bubble point pressure in the fluid [10].
3. The temporary stabilization is followed by continuous decline of the crack propagation speed and eventual arrest of the crack. As can be seen from Fig. 3, in the case of pure $CO_2$, the crack arrest length is *ca* 5.5 m, while adding 2% $CH_4$ extends the fracture to *ca* 8.5 m, and having *ca* 3.2% impurities in oxy-fuel stream results in a fracture of 15 m long, while adding 2% $H_2$ extends the fracture length beyond 16 m.

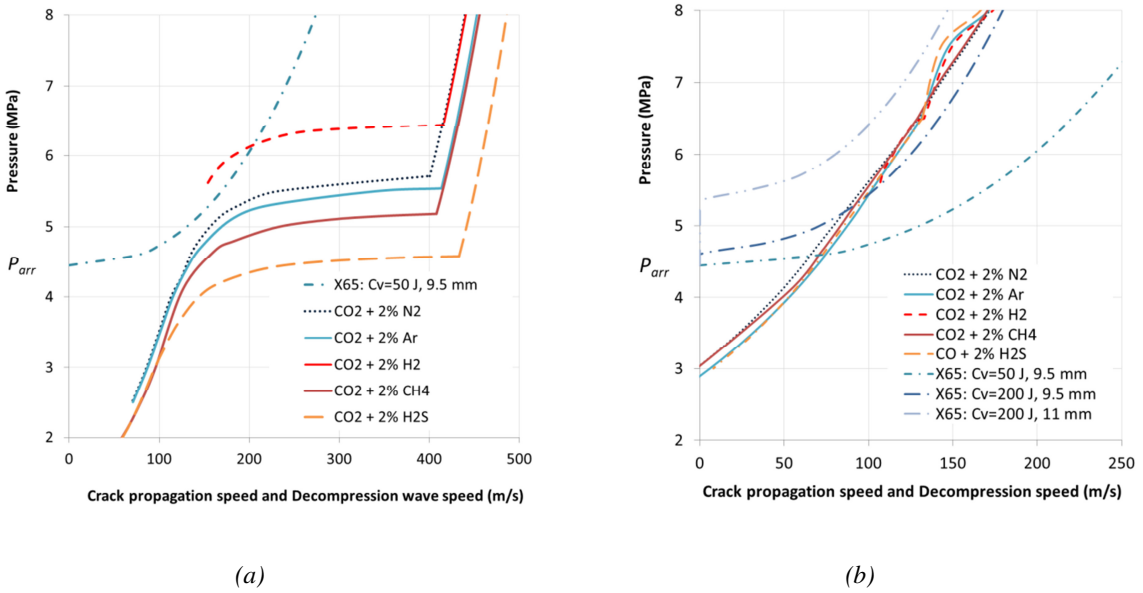


Fig. 4. Variation of the crack propagation speed predicted by equation (5) and the wave decompression speed described by equation (11) for the various $CO_2$ mixtures initially at 80 bar and 15 ºC *(a)* and 80 bar and 30 ºC *(b)*.

The above variations in the crack arrest length can be discussed in the context of BTC methodology, which is widely used in industry [16]. In BTC method the facture propagation or arrest are judged based on comparison of the crack speeds and the speed of decompression wave running in fluid. In particular, if the fluid pressure in the pipe is above the crack arrest pressure, $P_{arr}$, described by equation (6), the crack has potential to propagate. Furthermore,

the propagating crack will eventually arrest if the crack speed at a given pressure is less than the decompression speed:

$$u_{cr} < u_{dec} \tag{10}$$

The decompression wave speed can be calculated using using the following equation [9]:

$$u_{dec} = c_s - u = \int_{P}^{P_i} \frac{dP'}{\rho(P')c_s(P')} \tag{11}$$

where $u_{dec}$, $c_s$, $u$ and $P_i$ are respectively the decompression wave speed, the fluid isentropic speed of sound, the local velocity of the flow at the rupture plane and the initial pressure in the pipe prior to the fracture propagation.

In Fig. 4, *a* the crack propagation speed predicted by equation (5) for X65 steel with Cv=50J, is plotted along with the decompression wave speed calculated using equation (11) for various binary $CO_2$ mixtures carrying 2% (v/v) of impurities initially at 80 bar and 30 $^{o}$C. To evaluate the density and the speed of sound with the pressure along the isentropic decompression path in equation (11), GERG equation of state was used in REFPROP [34]. As can be further seen in Fig. 4, *a*, for all the mixtures except of $CO_2$ + 2%$H_2$, the decompression wave can be expected to run faster than the crack, eventually leading to the crack arrest once the fluid pressure will drop below the crack arrest pressure of *ca* 45 bar, as predicted by equation (6). Remarkably, despite the fact that the decompression curve for $CO_2$ + 2%$H_2$ mixture crosses the crack propagation curve, the coupled model predicted the fracture arrest (Fig. 3). This can be partially attributed to discrepancies in the physical properties of the fluid predicted by GERG and PC-SAFT equations of state.

Fig. 4, *b* shows the crack propagation speeds and the decompression wave speeds predicted for the various $CO_2$ mixtures transported in supercritical state at 80 bar and 30 $^{o}$C. Remarkably, the decompression wave speed at supercritical temperatures is not significantly affected by the presence of impurities. The crack propagation speeds are plotted for 0.5095 m internal diameter pipe made of X65 steel with the facture toughnesses $C_v$ of 50 and 200 J and the wall thicknesses of 9.45 and 11 mm. As can be seen, the wall thickness of 9.45 mm and $C_v$ = 50 J cannot guarantee the crack propagation speeds meeting the criterion (10) at the initial fluid pressures, as such posing a risk of uncontrolled running fracture. On the other hand, when using X65 steel with $C_v$ = 200 J and the wall thickness of 11 mm, the risk of uncontrolled fracture propagation can be eliminated.

### *3.2. Brittle fractures – Role of heat transfer*

This section describes the results of analysis of the temperature variation in vicinity of a pipeline rupture hole, based on numerical solution of the heat conduction equation for various conditions of heat exchange at the internal and external pipe walls, relevant to outflow of a low boiling point fluid from a small circular hole in a transportation pipeline. The study is performed for a medium-scale pipeline constructed using API X70 steel in CO2QUEST project for conducting $CO_2$ blowdown experiments [18]. Main specifications for the test section of the pipeline are summarized in Table 1.

Table 1. Main parameters of the pipeline section for the heat transfer study

| Parameter | Unit | Value |
|---|---|---|
| Pipeline internal diameter, $D$ | mm | 51 |
| Pipeline segment length | mm | 160 |
| Pipe wall thickness, $\delta_w$ | mm | 1.5 |
| Puncture diameter, $D_o$ | mm | 4 |
| Density of the steel pipe wall, $\rho_w$ | kg/m$^3$ | 7800 |
| Thermal conductivity of steel, $k_w$ | W/m/K | 43 |

In order to examine the impact of the heat transfer conditions at the pipe internal and external walls on the temperature distribution near the puncture hole, the heat transfer coefficients were varied over the ranges typical for convective heat transfer for a turbulent flow in a pipe and around a cylinder [31]. In particular, assuming that the pipeline is transporting dense-phase $CO_2$ stream at pressure around 100 bar, 20 $^oC$ temperature and velocities up to of *ca* 10 m/s, the heat transfer coefficient at the internal pipe wall, $h_{in}$, can be estimated at a maximum of *ca* 1000 W/m$^2$/K. Furthermore, the temperature in the bulk fluid surrounding the pipe is conservatively estimated to be –78 $^oC$, i.e. corresponding to the temperature at the normal sublimation point of $CO_2$. For a mixed convection around the pipe the maximum value of the heat transfer coefficient at the external pipe wall, $h_{ext}$, can be estimated to be *ca* 100 W/m$^2$/K.

Following the study by Saville *et al* [22], the pipe wall temperature at the circumference of the puncture hole was assumed to be equal to the saturation point of the fluid at the choked flow pressure. The latter may vary significantly during the pipeline decompression which can be simulated using the model described in Section 2.2. However, for the purpose of steady-state analysis in the present study, the temperature at the circumference of the puncture hole is considered as a model parameter, which for the sake of example was set to –50 $^oC$, i.e. in between the temperatures of the fluid inside and outside the pipe.

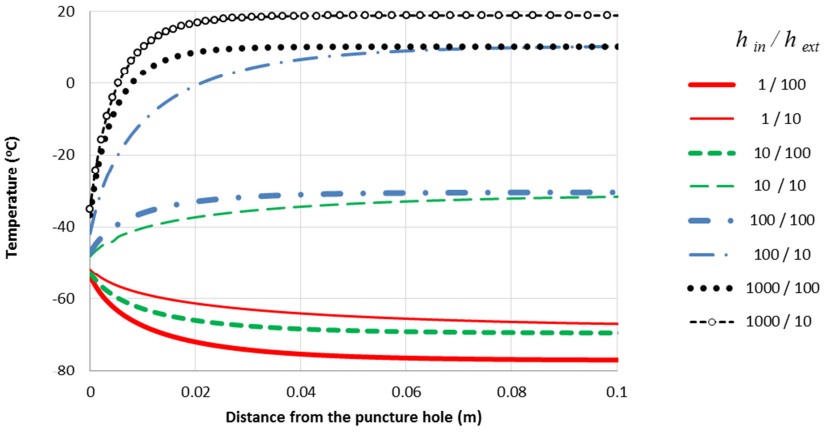


Fig. 5. Variation of temperature in vicinity of the crack for various combinations of the heat transfer coefficients $h_{in}$ and $h_{ext}$.

Fig. 5 shows the variation of the pipe wall temperature in vicinity of the puncture hole calculated for the various combinations of the heat transfer coefficients $h_{in}$ and $h_{ext}$. Note that in all the cases the temperature variation across the pipe wall was found to be relatively small compared to its variation along the pipeline.

As can be seen from Fig. 5, in cases where $h_{in} > h_{ext}$, i.e. the heat transfer inside the pipe is dominant, the pipe wall temperature increases with the distance from the hole. This is consistent with the temperature profiles predicted by Mahgerefteh and Atti [20] for scenarios of decompression of an overground pipeline, where the high intensity of heat transfer inside the pipe was due to relatively large transportation flowrate of the fluid. In these cases the pipe wall temperature is essentially limited by the temperature of the choked flow at the rupture hole. In the turn this means that these scenarios could pose a potential risk for brittle crack propagation only at late stages of decompression when the choked flow temperature could drop below the DBTT level (e.g. for X70 steel DBTT is –75 $^{o}$C [35], for which the saturation pressure of $CO_2$ is *ca* 1.4 bar).

Fig. 5 also shows that in those cases where the heat transfer inside the pipe is relatively slow compared to that around the pipe ($h_{in} < h_{ext}$), the wall temperature decreases with the distance from the puncture hole. These cases are particularly relevant to leaks from buried pipelines where expansion flow from the puncture hole envelops the pipe, resulting in high rates of cooling of the pipe wall. While the actual drop in the wall temperature depends on variation of the heat transfer and flow conditions in the vicinity of the puncture hole, the profiles presented in Fig. 6 show that the pipe wall temperature near the puncture hole may drop below the DBTT level even if the fluid at the puncture is relatively warm, increasing the risks of embrittlement of the pipe wall material at early stages of the pipeline decompression.

## 4. Conclusions

In this study a methodology is described for coupled modelling of an outflow, heat transfer and crack propagation in pipelines. The main constituent elements of the methodology include the transient dynamically-coupled FSI model of pipeline fracture propagation and model of heat transfer describing the temperature variation in the pipe wall in vicinity of the crack.

The FSI model was applied to study the pipeline fracture propagation and arrest upon the conditions relevant to the dense-phase and super-critical $CO_2$ pipeline transportation, covering temperatures from –15 to 45 $^{o}$C and accounting for up to *ca* 3% (v/v) of impurities in the transported $CO_2$ stream.

The study shows that the $CO_2$ stream impurities have a strong impact on the ductile fracture arrest distance in pipelines transporting dense-phase $CO_2$ at pressures above 80 bar and temperatures below *ca* 15 $^{o}$C. This effect is attributed to the impact of impurities on the fluid bubble-point pressure and the decompression speed. Particularly long fractures have been predicted for $CO_2$ mixtures containing $H_2$, and also the multicomponent mixture representative of the oxy-fuel capture. At the same time, given relatively low compressibility of dense-phase $CO_2$ the ductile fracture control could be achieved by choosing modern high-grade steels of sufficient material toughness ($C_v$ above *ca* 50 J) without use of crack arrestors.

On the other hand, at temperatures above *ca* 15 $^{o}$C and pressures near and above the $CO_2$ mixture cricondenbar pressure, the speed of decompression wave in the fluid may become lower than the speed of crack propagation in steel, increasing the chances of uncontrolled running fractures. This applies to warm and hot (supercritical) $CO_2$ streams of any purity where fracture arrestors would be required to minimize the chances of uncontrolled ductile fracture propagation.

To provide accurate estimation of the temperature variation in the vicinity of a pipeline leak, the heat conduction through the pipe wall was resolved using a finite element model. Implications of the flow and heat transfer conditions at the internal and external surfaces of the pipe wall for the brittle fracture propagation in overground and buried pipelines were discussed.

**Acknowledgements**

The research leading to the results contained in this paper received funding from the European Commission 7th Framework Programme FP7-ENERGY-2012-1 under grant number 309102 and Qatar National Research Fund (a member of The Qatar Foundation) NPRP award 8-1339-2-569. The paper reflects only the authors' views and the funders are not liable for any use that may be made of the information contained therein.

**References**

1. Doctor R, Palmer A, Coleman D, Davison J, Hendriks C, Kaarstad O, et al. Transport of CO2. IPCC Special Report on Carbon dioxide Capture and Storage. 2005.
2. Mohitpour M, Jenkins A, Nahas G, Pipeline T, Rock W, President V, et al. CO2 and greenhouse gas emissions. 2008;237–51.
3. Guo X, Yan X, Yu J, Zhang Y, Chen S, Mahgerefteh H, et al. Pressure response and phase transition in supercritical CO2 releases from a large-scale pipeline. Appl Energy [Internet]. 2016;178(2):189–97. Available from: http://linkinghub.elsevier.com/retrieve/pii/S0306261916308017
4. Wilkowski G, Maxey B. Fracture Initiation, Propagation and Arrest. In: 5th Symposium on Line Pipe Research November 1974. 1974.
5. Inoue T, Makino H, Endo S, Kubo T, Matsumoto T. Simulation method for shear fracture propagation in natural gas transmission pipelines. In: International Offshore and Polar engineering Conference. Honolulu, Hawaii, USA; 2003. p. 121–8.
6. Jones DG, Gough DW. Rich Gas Decompression Behavior in Pipelines. In: AGA-EPRG Linepipe Research Seminar IV, BRITISH GAS, Duisburg. 1981.
7. Makino H, Sugie T, Watanabe H, Kubo T, Shiwaku T, Endo S, et al. Natural Gas Decompression Behavior in High Pressure Pipelines. ISIJ Int [Internet]. 2001;41(4):389–95. Available from: http://joi.jlc.jst.go.jp/JST.Journalarchive/isijinternational1989/41.389?from=CrossRef
8. Aursand E, Aursand P, Berstad T, Dørum C, Hammer M, Munkejord ST, et al. CO2 Pipeline Integrity: A Coupled Fluid-structure Model Using a Reference Equation of State for CO2. Energy Procedia [Internet]. 2013 [cited 2014 Mar 2];37(1876):3113–22. Available from: http://linkinghub.elsevier.com/retrieve/pii/S1876610213004402
9. Aursand E, Dørum C, Hammer M, Morin A, Munkejord ST. CO2 pipeline integrity: Comparison of a coupled fluid-structure model and uncoupled two-curve methods. Energy Procedia. 2014;00:1–10.
10. Mahgerefteh H, Brown S, Denton G. Modelling the impact of stream impurities on ductile fractures in CO 2 pipelines. Chem Eng Sci [Internet]. 2012;74:200–10. Available from: http://dx.doi.org/10.1016/j.ces.2012.02.037
11. Munkejord ST, Jakobsen JP, Austegard A, Mølnvik MJ. Thermo- and fluid-dynamical modelling of two-phase multi-component carbon dioxide mixtures. Int J Greenh Gas Control. 2010;4(4):589–96.
12. Nordhagen HO, Kragset S, Berstad T, Morin a., Dørum C, Munkejord ST. A new coupled fluid–structure modeling methodology for running ductile fracture. Comput Struct [Internet]. 2012 Mar [cited 2014 Mar 2];94-95:13–21. Available from: http://linkinghub.elsevier.com/retrieve/pii/S0045794912000053
13. Mahgerefteh H, Oke AO, Rykov Y. Efficient numerical solution for highly transient flows. Chem Eng Sci [Internet]. 2006;61(15):5049–56. Available from: http://www.sciencedirect.com/science/article/pii/S0009250906001710
14. Makino H, Takeuchi I, Tsukamoto M, Kawaguchi Y. Study on the Propagating Shear Fracture in High Strength Line Pipes by Partial-gas Burst Test. ISIJ Int [Internet]. 2001;41(7):788–94. Available from: http://joi.jlc.jst.go.jp/JST.Journalarchive/isijinternational1989/41.788?from=CrossRef
15. Johnson DM, Horner N, Carlson L, Eiber RJ. Full scale validation of the fracture control of a pipeline designed to transport rich natural gas. Pipeline Technol. 2000;1:331–42.
16. Cosham A, Eiber RJ. Fracture propagation in CO2 pipelies. J Pipeline Eng. 2008;281–92.
17. Morin A, Kragset S, Munkejord ST. Pipeline flow modelling with source terms due to leakage: The straw

method. Energy Procedia [Internet]. 2012;23(1876):226–35. Available from: http://dx.doi.org/10.1016/j.egypro.2012.06.023
18. Porter RTJ, Mahgerefteh H, Brown S, Martynov S, Collard A, Woolley RM, et al. CO2QUEST: An overview of aims , objectives and main findings. Int J Greenh Gas Control. 2016;
19. Döbereiner, B. Münstermann S, Thibaux P. Analysis of slant fracture in the Battelle drop-weight tear test. In: 6th International Pipeline Technology Conference. Ostende, Belgien. Gent: Lab Soete; 2013. p. Paper no: S34–03.
20. Mahgerefteh H, Atti O. Modeling low-temperature-induced failure of pressurized pipelines. AIChE J. 2006;52(3):1248–56.
21. Cosham A, Koers R, Andrews R, Schmidt T. Progress Towards The New Eprg Recommendation For Crack Arrest Toughness For High Strength Line Pipe Steels. In: 20th JTM, 3-8 May 2015, Paris, France. 2015.
22. Saville G, Richardson SM, Barker P. Leakage in Ethylene Pipelines. Process Saf Environ Prot [Internet]. 2004;82(1):61–8. Available from: http://www.sciencedirect.com/science/article/pii/S0957582004711362
23. Talemi RH, Brown S, Martynov S, Mahgerefteh H. A hybrid fluid-structure interaction modelling of dynamic brittle fracture in pipeline steel transporting CO 2 streams. Int J Greenh Gas Control [Internet]. 2016; Available from: http://dx.doi.org/10.1016/j.ijggc.2016.08.021
24. Assessment of Hydrocarbon Transportation Pipelines. Qatar National Priority Research Progra. Project No. 8-1339-2-569. QNRF; 2014.
25. Mahgerefteh H, Brown S, Martynov S. A study of the effects of friction, heat transfer, and stream impurities on the decompression behavior in CO 2 pipelines. Greenh Gases Sci Technol [Internet]. 2012 Oct 24 [cited 2015 Sep 10];2(5):369–79. Available from: http://www.scopus.com/inward/record.url?eid=2-s2.0-84867518828&partnerID=tZOtx3y1
26. Chen NH. An Explicit Equation for Friction Factor in Pipe. Ind Eng Chem Fundam. 1979;18(3):296–7.
27. Diamantonis NI, Boulougouris GC, Mansoor E, Tsangaris DM, Economou IG. Evaluation of cubic, SAFT, and PC-SAFT equations of state for the vapor-liquid equilibrium modeling of CO2 mixtures with other gases. Ind Eng Chem Res. 2013;52:3933–42.
28. Brown S, Peristeras LD, Martynov S, Porter RTJ, Mahgerefteh H, Nikolaidis IK, et al. Thermodynamic interpolation for the simulation of two-phase flow of non-ideal mixtures. Comput Chem Eng [Internet]. 2016;95:49–57. Available from: http://dx.doi.org/10.1016/j.compchemeng.2016.09.005
29. LeVeque RJ. Finite Volume Methods for Hyperbolic Problems. Cambridge Univ Press [Internet]. 2002;54:258. Available from: http://books.google.com/books?hl=en&lr=&id=QazcnD7GUoUC&oi=fnd&pg=PR17&dq=Finite+Volume+Methods+for+Hyperbolic+Problems&ots=WXEzplVO1j&sig=vS0a-oIyjAnsZ8z-Mj_IkMJ_UHM
30. Brown S, Martynov S, Mahgerefteh H, Proust C. A homogeneous relaxation flow model for the full bore rupture of dense phase CO2 pipelines. Int J Greenh Gas Control [Internet]. 2013 Sep [cited 2015 Sep 10];17:349–56. Available from: http://www.scopus.com/inward/record.url?eid=2-s2.0-84879491859&partnerID=tZOtx3y1
31. Rohsenow WM, Hartnett JP, Cho YI. Handbook of Heat Transfer. 3rd ed. New York: McGrawHill,; 1998.
32. ABAQUS. Dassault Systemes. Abaqus/ CAE User's Guide. Providence, RI, USA: Dassault Systemes; 2013.
33. Porter RTJ, Fairweather M, Pourkashanian M, Woolley RM. The range and level of impurities in CO2 streams from different carbon capture sources. Int J Greenh Gas Control [Internet]. 2015;36:161–74. Available from: http://linkinghub.elsevier.com/retrieve/pii/S1750583615000705
34. Lemmon, M.L. Huber and MOM. NIST Reference Fluid Thermodynamic and Transport Properties - REFPROP, NIST Standard Reference Database 23. Applied Chemicals and Materials Division; 2013.
35. Hojjati-Talemi R, Cooreman S, Van Hoecke D. Finite element simulation of dynamic brittle fracture in pipeline steel: A XFEM-based cohesive zone approach. Proc Inst Mech Eng Part L J Mater Des Appl [Internet]. 2016;0(0):1–14. Available from: http://pil.sagepub.com/lookup/doi/10.1177/1464420715627379